Frontiers of Information Technology & Electronic Engineering
www.jzus.zju.edu.cn; engineering.cae.cn; www.springerlink.com
ISSN 2095-9184 (print); ISSN 2095-9230 (online)
E-mail: jzus@zju.edu.cn

Robust generalized sidelobe canceller based on eigenanalysis and a MaxSINR beamformer*

Quan-dong WANG[1,2], Liang-hao GUO[†‡1], Wei-yu ZHANG[1], Sui-ling REN[1], Chao YAN[1]

[1]*State Key Laboratory of Acoustics, Institute of Acoustics, Chinese Academy of Sciences, Beijing 100190, China*

[2]*University of Chinese Academy of Sciences, Beijing 100049, China*

[†]E-mail: glh2002@mail.ioa.ac.cn

Received June 9, 2017; Revision accepted Dec. 3, 2017; Crosschecked July 3, 2019

Abstract: A robust generalized sidelobe canceller is proposed to combat direction of arrival (DOA) mismatches. To estimate the interference-plus-noise (IPN) statistics characteristics, conventional signal of interest (SOI) extraction methods usually collect a large number of segments where only the IPN signal is active. To avoid that collection procedure, we redesign the blocking matrix structure using an eigenanalysis method to reconstruct the IPN covariance matrix from the samples. Additionally, a modified eigenanalysis reconstruction method based on the rank-one matrix assumption is proposed to achieve a higher reconstruction accuracy. The blocking matrix is obtained by incorporating the effective reconstruction into the maximum signal-to-interference-plus-noise ratio (MaxSINR) beamformer. It can minimize the influence of signal leakage and maximize the IPN power for further noise and interference suppression. Numerical results show that the two proposed methods achieve considerable improvements in terms of the output waveform SINR and correlation coefficients with the desired signal in the presence of a DOA mismatch and a limited number of snapshots. Compared to the first proposed method, the modified one can reduce the signal distortion even further.

Key words: Eigenanalysis; Interference-plus-noise covariance matrix reconstruction; Maximum signal-to-interference-plus-noise ratio criterion; Blocking matrix; Generalized sidelobe canceller; Direction of arrival mismatch
https://doi.org/10.1631/FITEE.1700367 **CLC number:** TN911.72

1 Introduction

In noisy environments, the signal of interest (SOI) is always masked by the strong background noise and interference which are near the source, resulting in difficulty with subsequent target localization and recognition. To extract the SOI, considerable effort has been made in adaptive beamforming in the past decades (van Trees, 2002; Li and Stoica, 2005). However, adaptive beamforming is very sensitive to model mismatches, i.e., covariance matrix mismatch and steering vector (SV) mismatch. One type of robust beamforming used widely is the generalized sidelobe canceller (GSC). The standard GSC is usually composed of three building blocks: a fixed beamformer which produces an enhanced desired signal reference, a blocking matrix which produces a noise-only reference by blocking the desired signal, and an unconstrained adaptive noise canceller (ANC) which attempts to cancel the residual noise in the output of the fixed beamformer.

Griffiths and Jim (1982) altered the linearly constrained minimum variance (LCMV) beamformer to the GSC as an unconstrained adaptive beamformer. However, its performance depends on the estimated direction of arrival (DOA). In the case of a DOA mismatch, the blocking matrix cannot produce a

‡ Corresponding author

* Project supported by the National Natural Science Foundation of China (No. 61571436)

ORCID: Quan-dong WANG, http://orcid.org/0000-0001-8775-1437

noise-only reference, and thus it causes signal cancellation and decreases the amount of interference suppression.

Several techniques have been proposed to improve the robustness of the GSC. To minimize the signal leakage, an adaptive blocking matrix with constrained filter coefficients was proposed to cope with DOA mismatch (Hoshuyama et al., 1999). However, updates of the adaptive blocking matrix have to be carried out in the case of a high signal-to-interference ratio (SIR). To obtain better robustness, the ratios of different pairs of transfer function are estimated using the signal non-stationarity and used to replace the SVs in the blocking matrix (Gannot et al., 2001; Talmon et al., 2009). Several adaptive blocking matrices were compared to analyze the performance of the robust GSCs in Herbordt and Kellermann (2002). The GSC in Warsitz et al. (2008) used a blocking matrix based on generalized eigenvalue decomposition (GEVD), and the weight vector of its fixed beamformer was determined according to the maximum signal-to-interference-plus-noise ratio (MaxSINR) criterion (Warsitz and Haeb-Umbach, 2007). It does not need a priori knowledge of the array structure and the DOA, and its good robustness relies only on the interference-plus-noise (IPN) covariance matrix estimation. A novel GSC structure in Habets and Benesty (2013) also depends on the IPN covariance matrix to manage a tradeoff between the suppression of interference and background noise. With sparse coding, the interference reference is extracted precisely to cancel the residual noise (Yang and Qian, 2014). Prior to signal extraction, these methods require a preprocessing technique, such as voice activity detection (VAD), to detect and collect a large number of segments where only the IPN signal is active. However, these preprocessing techniques are unavailable or inaccurate in many scenarios due to the strong background noise.

Other categories of robust beamforming include the multichannel Wiener filter beamformer (Spriet et al., 2004; Doclo et al., 2007; Souden et al., 2010; Cornelis et al., 2011), minimum variance distortionless response (MVDR) (Capon, 1969; Li and Stoica, 2005; Du et al., 2010), and LCMV beamformers (Buckley, 1987; Zhang and Thng, 2002; Zhao et al., 2011). Recently, several covariance matrix reconstruction methods have been proposed to be applied in the MVDR beamformers to get rid of the SOI component. These methods can make the beamformer less sensitive to the DOA mismatch. In Gu and Leshem (2012), the IPN covariance matrix was reconstructed by exploiting the Capon spatial spectrum for integration over a direction range where the direction of the SOI was excluded. Furthermore, the SVs of the interference are constrained by an uncertainty set for the robustness against array geometry mismatches (Huang et al., 2015). These improvements against the mismatches are superior but highly dependent on the spatial power spectrum density estimation.

To reduce the complexity of the integration methods, a number of methods have been investigated. A sparse method was presented in Gu et al. (2014). A simplified method has also been suggested (Chen et al., 2015; Shen et al., 2015; Gong et al., 2017). It reconstructs the IPN covariance matrix by removing the SOI eigenvalue whose corresponding eigenvector has the maximum correlation coefficient with the estimated SV. Inspired by the sampling theorem, a spatial power spectrum sampling technique was proposed in Zhang ZY et al. (2016) to structure the IPN covariance matrix at a lower level of complexity. Instead of the Capon spatial spectrum, the beamformer based on an iterative adaptive approach (IAA) was carried out in Wang et al. (2016) to estimate the spatial spectrum for the reconstruction. Unfortunately, the spatial spectrum density estimation remains inaccurate in this type of approach.

Another trend for achieving the reconstruction is to estimate the SV of the SOI or every interference source. In Zhang YP et al. (2016), the SV of the SOI was estimated by maximizing the output power of the MVDR beamformer, and then the SOI part was removed from the sample covariance matrix to reconstruct the IPN covariance matrix. However, the improvement in low SNR scenarios is very limited. Each interference SV and the corresponding interference covariance matrix were estimated by integrating over the separate interference angular sector (Yuan and Gan, 2016; Qian et al., 2017). Then, the IPN covariance matrix was reconstructed using these estimates. In practice, however, neither the number of interfer-

ence signals nor the DOA of every source is known.

Except for the above integration methods, the subspace methods in robust adaptive beamformers have also been investigated to address the mismatches (Feldman, 1996; Huang et al., 2012; Jia et al., 2013; Ren et al., 2015; Chen et al., 2016; Li et al., 2016; Yuan and Gan, 2017). In Shen et al. (2015), a novel subspace method was proposed to estimate the SV of the SOI from the common part of two subspaces. This method was used well in Yuan and Gan (2017) to estimate all the interference SVs to obtain the IPN covariance matrix. To calibrate the SV, a projection matrix corresponding to the SOI subspace is estimated by constraining the number of large eigenvalues with a fixed threshold (Feldman, 1996; Huang et al., 2012; Jia et al., 2013). However, the number of sources is usually unavailable. A more recent approach in this category (Ren et al., 2015) is to build a robust power ratio to determine the eigenvectors not dominated by the SOI, and then to subtract them from the sample covariance matrix. It improves the robustness and requires a small number of snapshots.

In this paper, we propose a GSC with an advanced blocking matrix structure, which is robust against a DOA mismatch. In this structure, two IPN covariance matrix reconstruction methods are employed to save the collection process of the IPN signal. One is the basic eigenanalysis method formulated in Section 3.1.2. The other is a rank-one assumption-based version, where the number of eigenvectors for the SOI is constrained as one to improve the accuracy of IPN covariance matrix estimation. Then the blocking matrix is calculated using the MaxSINR beamformer weight vector, which is obtained from an accurate reconstruction and a projection vector. It minimizes the signal leakage and maximizes the noise and interference power. The proposed methods not only require a smaller number of snapshots, but also obtain better robustness.

2 Signal model

We consider an array with M omnidirectional sensors with spacing d. Assume that there are J signals arriving from separated directions ϕ_p, p=0, 1, ..., J−1. In the short-time Fourier transform (STFT) domain the received array data $\boldsymbol{X}(\omega_l, k)$ can be shown as

$$\begin{aligned}\boldsymbol{X}(\omega_l,k)&=\begin{bmatrix}\boldsymbol{a}(\omega_l,\phi_0)\\ \boldsymbol{a}(\omega_l,\phi_1)\\ \vdots\\ \boldsymbol{a}(\omega_l,\phi_{J-1})\end{bmatrix}^{\mathrm{T}}\begin{bmatrix}s_0(\omega_l,k)\\ s_1(\omega_l,k)\\ \vdots\\ s_{J-1}(\omega_l,k)\end{bmatrix}+\boldsymbol{N}(\omega_l,k)\\ &=\boldsymbol{A}(\omega_l)\boldsymbol{S}(\omega_l,k)+\boldsymbol{N}(\omega_l,k),\\ &\quad l=1,2,...,L,\end{aligned}\tag{1}$$

where $(\cdot)^{\mathrm{T}}$ denotes the transpose, L is the number of frequency bins, l and k denote the frequency and block indices respectively, and $s_j(\omega_l, k)$ and $\boldsymbol{a}(\omega_l, \phi_j) \in \mathbb{C}^M$ are the j^{th} source and the associated SV, respectively. $\boldsymbol{S}(\omega_l, k)$ is the vector of J statistically independent stationary sources, $\boldsymbol{A}(\omega_l, k)$ consists of the SVs for all sources, and $\boldsymbol{N}(\omega_l, k)$ is the additive Gaussian noise vector.

The frequency-domain sample covariance matrix $\boldsymbol{R}_{\boldsymbol{X}}(\omega_l, k)$ is approximately calculated with K snapshots in the k^{th} block at frequency ω_l. Its estimation $\bar{\boldsymbol{R}}_X(\omega_l,k)$ with the eigenvalue decomposition can be written as

$$\begin{aligned}\bar{\boldsymbol{R}}_{\boldsymbol{X}}(\omega_l,k)&=\frac{1}{K}\sum_{t=0}^{K-1}\boldsymbol{X}(\omega_l,k-t)\boldsymbol{X}^{\mathrm{H}}(\omega_l,k-t)\\ &=\sum_{m=1}^{M}\lambda_m(\omega_l,k)\boldsymbol{v}_m(\omega_l,k)\boldsymbol{v}_m^{\mathrm{H}}(\omega_l,k),\\ &\quad l=1,2,...,L,\end{aligned}\tag{2}$$

where $(\cdot)^{\mathrm{H}}$ denotes the conjugate transpose, and $\lambda_m(\omega_l, k)$ and $\boldsymbol{v}_m(\omega_l, k)$ denote the m^{th} eigenvalue and the corresponding eigenvector of $\bar{\boldsymbol{R}}_X(\omega_l,k)$ respectively.

3 Proposed methods

The structure diagram of the proposed robust GSC is shown in Fig. 1. The structure contains five building blocks. The conventional beamformer (CBF) is chosen as the fixed beamformer to produce an SOI reference. Its output $Y_{\mathrm{FB}}(\omega_l, k)$ is formulated as

$$\begin{aligned}Y_{\mathrm{FB}}(\omega_l,k)&=\boldsymbol{F}_{\mathrm{FB}}^{\mathrm{H}}(\omega_l,k)\boldsymbol{X}(\omega_l,k)\\ &=\frac{\bar{\boldsymbol{a}}^{\mathrm{H}}(\omega_l,\bar{\phi}_{\mathrm{SOI}})}{M}\boldsymbol{X}(\omega_l,k),\quad l=1,2,...,L,\end{aligned}\tag{3}$$

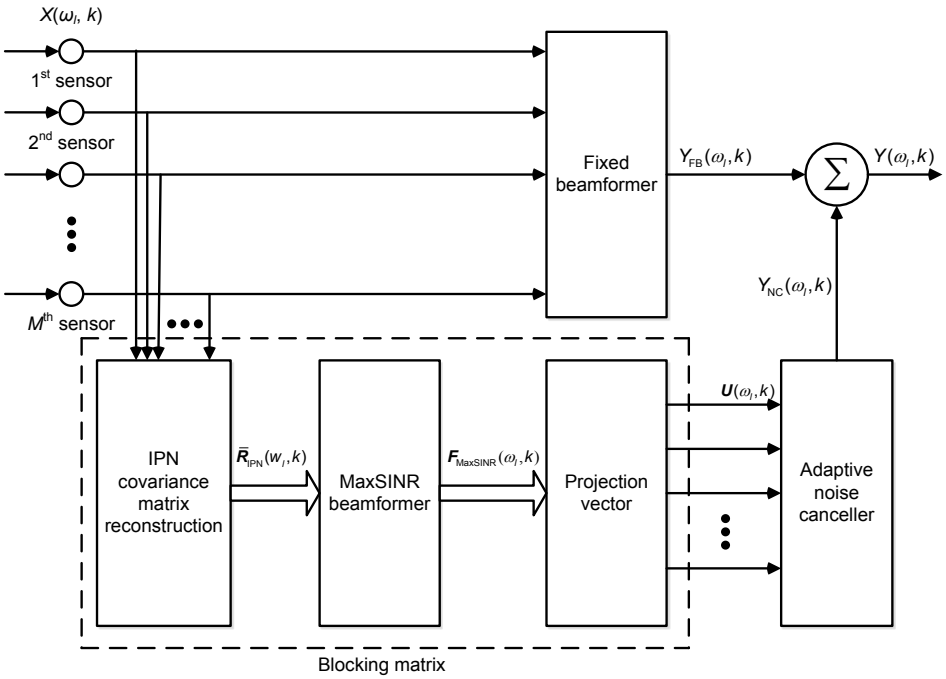

Fig. 1 The proposed generalized sidelobe canceller structure

where $\boldsymbol{F}_{\mathrm{FB}}(\omega_l, k)$ is the weight vector of CBF and $\bar{\boldsymbol{a}}(\omega_l, \bar{\phi}_{\mathrm{SOI}})$ is the presumed SV calculated from the array structure and the DOA of the SOI. The redesigned robust blocking matrix is constituted by three blocks. The IPN covariance matrix reconstruction block eliminates the SOI components. The MaxSINR beamformer block and the projection vector block work together to produce the IPN-only reference. The normalized least mean square (NLMS) ANC attempts to cancel the residual noise in the SOI reference.

3.1 Interference-plus-noise covariance matrix reconstruction

3.1.1 Capon spatial spectrum integration and IPN covariance matrix reconstruction

A method widely used to reconstruct the IPN covariance matrix is to use the Capon spatial spectrum estimator:

$$\bar{P}(\omega_l,\phi,k)=\frac{1}{\bar{\boldsymbol{a}}^{\mathrm{H}}(\omega_l,\phi)\bar{\boldsymbol{R}}_X^{-1}(\omega_l,k)\bar{\boldsymbol{a}}(\omega_l,\phi)},\quad l=1,2,...,L, \tag{4}$$

which is the spatial power spectrum of the Capon beamformer (Capon, 1969). Using the estimator, we reconstruct the IPN covariance matrix $\bar{\boldsymbol{R}}_{\mathrm{IPN}}(\omega_l,k)$ as (Gu and Leshem, 2012)

$$\begin{aligned}\bar{\boldsymbol{R}}_{\mathrm{IPN}}(\omega_l,k)&=\int_{\Theta_{\mathrm{IPN}}}\bar{P}(\omega_l,\phi,k)\bar{\boldsymbol{a}}(\omega_l,\phi)\bar{\boldsymbol{a}}^{\mathrm{H}}(\omega_l,\phi)\,\mathrm{d}\phi\\&=\int_{\Theta_{\mathrm{IPN}}}\frac{\bar{\boldsymbol{a}}(\omega_l,\phi)\bar{\boldsymbol{a}}^{\mathrm{H}}(\omega_l,\phi)}{\bar{\boldsymbol{a}}^{\mathrm{H}}(\omega_l,\phi)\bar{\boldsymbol{R}}_X^{-1}(\omega_l,k)\bar{\boldsymbol{a}}(\omega_l,\phi)}\mathrm{d}\phi,\\&\quad l=1,2,...,L.\end{aligned} \tag{5}$$

Here, Θ_{IPN} is an angular sector where the interference signals are located, and Θ_{SOI} is the complement of Θ_{IPN} where the SOI is located. The requirement of Θ_{SOI} is more relaxed than that of the accurate DOA of the SOI, and it can be obtained with low-resolution orientation methods (Gu and Leshem, 2012). The performance of this method depends on the number of snapshots. Given a small number of snapshots, there will be a large deviation between $\bar{\boldsymbol{R}}_X(\omega_l,k)$ and $\boldsymbol{R}_{\boldsymbol{X}}(\omega_l, k)$, resulting in an inaccurate estimation of the Capon spatial spectrum and imprecise IPN covariance matrix reconstruction. Moreover, when the number of snapshots is smaller than that of the sensors, $\bar{\boldsymbol{R}}_X(\omega_l,k)$ is singular.

Under these circumstances, we develop an

eigenanalysis-based method and propose a modified approach for IPN covariance matrix reconstruction using the presumed SVs and Θ_{SOI}.

3.1.2 Basic eigenanalysis and IPN covariance matrix reconstruction

To reconstruct the IPN covariance matrix, the eigenvalue decomposition on $\bar{\boldsymbol{R}}_X(\omega_l,k)$ should be taken first. Then, the CBF spatial spectrum $\mathrm{BV}_m(\omega_l, \phi, k)$ of an eigenvector $\boldsymbol{v}_m(\omega_l, k)$ can be calculated as (Ren et al., 2015)

$$\begin{aligned}&\mathrm{BV}_m(\omega_l,\phi,k)\\&\quad=\bar{\boldsymbol{a}}^{\mathrm{H}}(\omega_l,\phi)\boldsymbol{v}_m(\omega_l,k)\boldsymbol{v}_m^{\mathrm{H}}(\omega_l,k)\bar{\boldsymbol{a}}(\omega_l,\phi),\\&\quad m=1,2,...M,\ l=1,2,...,L.\end{aligned}\tag{6}$$

Here, a power ratio PR_m aiming to determine which eigenvectors is dominated by the SOI is defined as

$$\begin{aligned}&\mathrm{PR}_m=\frac{\max\limits_{\phi\in\Theta_{\mathrm{SOI}}}\mathrm{BV}_m(\omega_l,\phi,k)}{\max\limits_{\phi\in[-90^\circ,90^\circ]}\mathrm{BV}_m(\omega_l,\phi,k)},\\&m=1,2,...,M,\ l=1,2,...,L.\end{aligned}\tag{7}$$

PR_m denotes the ratio between the maximum of the CBF power spectrum of $\boldsymbol{v}_m(\omega_l, k)$ in Θ_{SOI} and the maximum in the whole direction region. It means $\mathrm{PR}_m\leq 1$. Its detailed properties were presented in Ren et al. (2015). If $\mathrm{PR}_m\geq\gamma$ where γ denotes the threshold, the corresponding $\boldsymbol{v}_m(\omega_l, k)\in\boldsymbol{U}_{\mathrm{SOIP}}(\omega_l, k)$, where $\boldsymbol{U}_{\mathrm{SOIP}}(\omega_l, k)$ denotes the subspace dominated by the SOI and partial noise components. In contrast, if $\mathrm{PR}_m<\gamma$, $\boldsymbol{v}_m(\omega_l, k)\in\boldsymbol{U}_{\mathrm{IPN}}(\omega_l, k)$, where $\boldsymbol{U}_{\mathrm{IPN}}(\omega_l, k)$ represents the subspace dominated by the interference signals and noise components. Then, we have the decision criteria as

$$\begin{aligned}&\begin{cases}\mathrm{PR}_m<\gamma\Rightarrow\boldsymbol{v}_m(\omega_l,k)\in\boldsymbol{U}_{\mathrm{IPN}}(\omega_l,k),\\\mathrm{PR}_m\geq\gamma\Rightarrow\boldsymbol{v}_m(\omega_l,k)\in\boldsymbol{U}_{\mathrm{SOIP}}(\omega_l,k),\end{cases}\\&\quad m=1,2,...,M,l=1,2,...,L,\end{aligned}\tag{8}$$

where γ=1 is set in an ideal condition.

Now, the IPN covariance matrix can be reconstructed as

$$\begin{aligned}&\bar{\boldsymbol{R}}_{\mathrm{IPN}}(\omega_l,k)=\boldsymbol{P}_\perp(\omega_l,k)\bar{\boldsymbol{R}}_X(\omega_l,k)\boldsymbol{P}_\perp^{\mathrm{H}}(\omega_l,k),\\&\quad l=1,2,...,L,\end{aligned}\tag{9}$$

where $\boldsymbol{P}_\perp(\omega_l,k)=\boldsymbol{U}_{\mathrm{IPN}}(\omega_l,k)\boldsymbol{U}_{\mathrm{IPN}}^{\mathrm{H}}(\omega_l,k)$ is the projection matrix.

In practice, when the number of interference signals or the interference power is extremely large, the power leakage will become serious between the SOI subspace and the IPN subspace. It results in an inaccurate CBF power spectrum $\mathrm{BV}_m(\omega_l, \phi, k)$ and also causes $\mathrm{PR}_m<1$ though the corresponding eigenvector actually belongs to $\boldsymbol{U}_{\mathrm{SOIP}}(\omega_l, k)$. Consequently, it is reasonable to choose a threshold γ lower than 1, e.g., 0.7, to ensure that the SOI eigenvector is in $\boldsymbol{U}_{\mathrm{SOIP}}(\omega_l, k)$. When γ<1, however, some eigenvectors belonging to the noise or interference signals can meet the decision criteria to be included in $\boldsymbol{U}_{\mathrm{SOIP}}(\omega_l, k)$, and will cause the amount of signal distortion to increase and the amount of interference suppression to be reduced.

3.1.3 Modified eigenanalysis and IPN covariance matrix reconstruction

To overcome the above problem, we propose a modified eigenanalysis method here. In the case of single target source extraction, the received SOI vector $\boldsymbol{X}_{\mathrm{S}}(\omega_l, k)$ can be expressed as

$$\boldsymbol{X}_{\mathrm{S}}(\omega_l,k)=\boldsymbol{a}(\omega_l,\phi_{\mathrm{SOI}})s_{\mathrm{SOI}}(\omega_l,k),\ l=1,2,...,L,\tag{10}$$

where $s_{\mathrm{SOI}}(\omega_l, k)$ denotes the waveform of the SOI in the STFT domain and $\boldsymbol{a}(\omega_l, \phi_{\mathrm{SOI}})$ is the actual SV of the SOI.

Obviously, the SOI covariance matrix $\boldsymbol{R}_{\mathrm{SOI}}(\omega_l, k)$ is a rank-one matrix (Souden et al., 2010; Zhu et al., 2016):

$$\begin{aligned}&\boldsymbol{R}_{\mathrm{SOI}}(\omega_l,k)=P_{\mathrm{s}}(\omega_l,k)\boldsymbol{a}(\omega_l,\phi_{\mathrm{SOI}})\boldsymbol{a}^{\mathrm{H}}(\omega_l,\phi_{\mathrm{SOI}}),\\&\quad l=1,2,...,L,\end{aligned}\tag{11}$$

where $P_{\mathrm{s}}(\omega_l,k)=E\{|s_{\mathrm{SOI}}(\omega_l,k)|^2\}$ is the power spectrum density of the SOI.

Therefore, we constrain the number of eigenvectors in $\boldsymbol{U}_{\mathrm{SOI}}(\omega_l, k)$ as one, and the decision criterion is modified as

$$\begin{cases} \mathrm{PR}_m \geq \gamma \Rightarrow \boldsymbol{v}_m(\omega_l,k) \in \boldsymbol{U}_{\mathrm{SOIP}}(\omega_l,k), \\ \quad \Rightarrow \begin{cases} \underset{\boldsymbol{v}_m(\omega_l,k)}{\operatorname{argmax}} \max\limits_{\phi \in \Theta_{\mathrm{SOI}}} \mathrm{BV}_m(\omega_l,\phi,k) \in \boldsymbol{U}_{\mathrm{SOI}}(\omega_l,k), \\ \text{others} \in \boldsymbol{U}_{\mathrm{IPN}}(\omega_l,k), \end{cases} \\ \mathrm{PR}_m < \gamma \Rightarrow \boldsymbol{v}_m(\omega_l,k) \in \boldsymbol{U}_{\mathrm{IPN}}(\omega_l,k), \\ m=1,2,...,M,\ l=1,2,...,L. \end{cases} \tag{12}$$

It is obvious that the exact eigenvector of the SOI has the maximum power spectral density in Θ_{SOI}. Thus, after including all possible SOI eigenvectors in $\boldsymbol{U}_{\mathrm{SOIP}}(\omega_l, k)$ with a given threshold, this method rebuilds the SOI subspace by selecting the one with the maximum power spectrum density in Θ_{SOI}. It manages a good balance between SOI distortion and interference suppression, because it discards very limited SOI power and keeps the interference and noise components for more accurate reconstruction. Note that if the bearing interval between the interference and SOI is less than the 3 dB main-lobe bandwidth of the CBF beam pattern, eigenvalue decomposition cannot distinguish the SOI from the interference. In this extreme condition, the SOI and the IPN will share the same subspace.

3.2 MaxSINR beamformer and blocking matrix

Leveraging the IPN covariance matrix reconstruction, we can design the robust blocking matrix with the MaxSINR beamformer.

3.2.1 MaxSINR beamformer

The MaxSINR beamformer aims to maximize the SINR at the beamformer output (Warsitz and Haeb-Umbach, 2007). Its weight vector $\boldsymbol{F}_{\mathrm{MaxSINR}}(\omega_l, k)$ can be modeled as

$$\begin{aligned} &\boldsymbol{F}_{\mathrm{MaxSINR}}(\omega_l,k) \\ &= \arg\max_{\boldsymbol{F}(\omega_l,k)} \frac{\boldsymbol{F}^{\mathrm{H}}(\omega_l,k)\boldsymbol{R}_{\mathrm{SOI}}(\omega_l,k)\boldsymbol{F}(\omega_l,k)}{\boldsymbol{F}^{\mathrm{H}}(\omega_l,k)\boldsymbol{R}_{\mathrm{IPN}}(\omega_l,k)\boldsymbol{F}(\omega_l,k)} \\ &= \arg\max_{\boldsymbol{F}(\omega_l,k)} \frac{\boldsymbol{F}^{\mathrm{H}}(\omega_l,k)\boldsymbol{R}_{\boldsymbol{X}}(\omega_l,k)\boldsymbol{F}(\omega_l,k)}{\boldsymbol{F}^{\mathrm{H}}(\omega_l,k)\boldsymbol{R}_{\mathrm{IPN}}(\omega_l,k)\boldsymbol{F}(\omega_l,k)}, \\ &\qquad l=1,2,...,L, \end{aligned} \tag{13}$$

where $\boldsymbol{R}_X(\omega_l, k)=\boldsymbol{R}_{\mathrm{SOI}}(\omega_l, k)+\boldsymbol{R}_{\mathrm{IPN}}(\omega_l, k)$.

The GEVD of the matrix pair $(\bar{\boldsymbol{R}}_X(\omega_l,k), \bar{\boldsymbol{R}}_{\mathrm{IPN}}(\omega_l,k))$ is used to obtain the optimal solution (Warsitz and Haeb-Umbach, 2007):

$$\begin{aligned} &\bar{\boldsymbol{R}}_{\boldsymbol{X}}(\omega_l,k)\boldsymbol{F}(\omega_l,k) = \lambda(\omega_l,k)\bar{\boldsymbol{R}}_{\mathrm{IPN}}(\omega_l,k)\boldsymbol{F}(\omega_l,k), \\ &\qquad l=1,2,...,L, \end{aligned} \tag{14}$$

where $\bar{\boldsymbol{R}}_X(\omega_l,k)$ is obtained by Eq. (2). $\bar{\boldsymbol{R}}_{\mathrm{IPN}}(\omega_l,k)$ is usually estimated by a preprocess block with a large number of segments containing only the IPN signal. Alternatively, it can be calculated using a priori knowledge of the noise and the interference signals (Wang et al., 2015). However, the preprocessing is not accurate in the presence of strong noise and interference signals, and a priori knowledge is usually unavailable in practice. To overcome the above problems, $\bar{\boldsymbol{R}}_{\mathrm{IPN}}(\omega_l,k)$ can be extracted from Eqs. (6), (7), (9), and (12). Leveraging the IPN co-variance matrix reconstruction, we can obtain the optimal weight vector of the MaxSINR beamformer as

$$\boldsymbol{F}_{\mathrm{MaxSINR}}(\omega_l,k) = \eta \boldsymbol{F}_{\mathrm{max\_eig}}(\omega_l,k),\ \ l=1,2,...,L, \tag{15}$$

where η is an arbitrary nonzero complex constant and $\boldsymbol{F}_{\mathrm{max\_eig}}(\omega_l, k)$ is the generalized eigenvector with the largest eigenvalue of Eq. (14). Then the output of the beamformer can be obtained as

$$\begin{aligned} &Y_{\mathrm{MaxSINR}}(\omega_l,k) = \boldsymbol{F}^{\mathrm{H}}_{\mathrm{MaxSINR}}(\omega_l,k)\boldsymbol{X}(\omega_l,k), \\ &\qquad l=1,2,...,L. \end{aligned} \tag{16}$$

Since no distortionless constraints are used by the MaxSINR beamformer, the output will not be used as the SOI reference, while it can be used to construct the blocking matrix.

3.2.2 Projection vector and blocking matrix

The $M\times(M-1)$ blocking matrix of the standard GSC $\boldsymbol{B}_{\mathrm{s}}(\omega_l, \bar{\phi}_{\mathrm{SOI}})$ uses the assumed SV of the SOI to subtract pairs of input data, and it is simply constructed as follows:

$$\begin{aligned} &\boldsymbol{B}_{\mathrm{s}}(\omega_l,\bar{\phi}_{\mathrm{SOI}}) \\ &= \begin{bmatrix} -1, & -1, & \cdots & -1 \\ \mathrm{e}^{-\mathrm{j}\omega_l\tau_2(\bar{\phi}_{\mathrm{SOI}})}, & 0 & \cdots & 0 \\ 0 & \mathrm{e}^{-\mathrm{j}\omega_l\tau_3(\bar{\phi}_{\mathrm{SOI}})} & \cdots & 0 \\ \vdots & \vdots & & \vdots \\ 0 & 0 & \cdots & \mathrm{e}^{-\mathrm{j}\omega_l\tau_M(\bar{\phi}_{\mathrm{SOI}})} \end{bmatrix}, \\ &\qquad l=1,2,...,L, \end{aligned} \tag{17}$$

where τ_i (i=2, 3, ..., M) is the propagation delay between the i^{th} sensor and the reference sensor. Its performance will decrease significantly when there is DOA mismatch.

To mitigate the influence of the DOA mismatch, the blocking matrix is redesigned using the MaxSINR beamformer. As the noise reference vector $\boldsymbol{U}(\omega_l, k)$ is orthogonal to the SOI, $\boldsymbol{U}(\omega_l, k)$ is approximately orthogonal to the output of the MaxSINR beamformer $Y_{\text{MaxSINR}}(\omega_l, k)$:

$$E[U(\omega_l,k)Y^*_{\text{MaxSINR}}(\omega_l,k)]\approx 0,\quad l=1,2,...,L, \tag{18}$$

where $E[\cdot]$ denotes the function of mathematical expectation, and the symbol $(\cdot)^*$ denotes the conjugate of a variable. In this case, a projection vector $\boldsymbol{P}(\omega_l, k)$ can be designed to produce the noise-only reference $\boldsymbol{U}(\omega_l, k)$ (Warsitz et al., 2008):

$$\boldsymbol{U}(\omega_l,k)=\boldsymbol{X}(\omega_l,k)-\boldsymbol{P}(\omega_l,k)Y_{\text{MaxSINR}}(\omega_l,k),\quad l=1,2,...,L. \tag{19}$$

Substituting Eqs. (16) and (19) into Eq. (18), we have

$$\boldsymbol{P}(\omega_l,k)=\frac{\bar{\boldsymbol{R}}_{\boldsymbol{X}}(\omega_l,k)\boldsymbol{F}_{\text{MaxSINR}}(\omega_l,k)}{\boldsymbol{F}^{\text{H}}_{\text{MaxSINR}}(\omega_l,k)\bar{\boldsymbol{R}}_{\boldsymbol{X}}(\omega_l,k)\boldsymbol{F}_{\text{MaxSINR}}(\omega_l,k)},\quad l=1,2,...,L. \tag{20}$$

Rewriting $\boldsymbol{U}(\omega_l, k)=\boldsymbol{B}^{\text{H}}(\omega_l, k)\boldsymbol{X}(\omega_l, k)$, the blocking matrix $\boldsymbol{B}(\omega_l, k)$ is obtained as

$$\boldsymbol{B}^{\text{H}}(\omega_l,k)=\boldsymbol{I}_M-\boldsymbol{P}(\omega_l,k)\boldsymbol{F}^{\text{H}}_{\text{MaxSINR}}(\omega_l,k),\quad l=1,2,...,L. \tag{21}$$

Essentially, $\boldsymbol{B}(\omega_l, k)$ produces the noise reference under the minimum SINR criterion, since the MaxSINR beamformer optimal weight vector is projected to remove the SOI component. Therefore, it can minimize the signal leakage and maximize the noise and interference power for further noise and interference suppression.

3.3 NLMS-based ANC

Given the fixed beamformer and the robust blocking matrix, we have two references: one is the SOI reference $Y_{\text{FB}}(\omega_l, k)$, which is composed of both the SOI waveform and the residual noise; the other is the IPN-only reference $\boldsymbol{U}(\omega_l, k)$. To eliminate the residual noise under the distortionless constraint, the multichannel Wiener filter $\boldsymbol{G}(\omega_l, k)$ is designed to minimize the output power:

$$\begin{aligned}E\left\{\left|Y(\omega_l,k)\right|^2\right\}&=E\left\{\left|Y_{\text{FB}}(\omega_l,k)-Y_{\text{NC}}(\omega_l,k)\right|^2\right\}\\&=E\left\{\left|Y_{\text{FB}}(\omega_l,k)-\boldsymbol{G}^{\text{H}}(\omega_l,k)\boldsymbol{U}(\omega_l,k)\right|^2\right\},\\&\qquad l=1,2,...,L,\end{aligned} \tag{22}$$

where $Y_{\text{NC}}(\omega_l, k)$ is the multichannel Wiener filter output and $Y(\omega_l, k)$ is the GSC output.

Considering the computational complexity, we prefer the NLMS algorithm in Haykin (2010) to the Wiener solution. The filter is updated block by block in the frequency domain:

$$\boldsymbol{G}(\omega_l,k+1)=\boldsymbol{G}(\omega_l,k)+\mu\frac{\boldsymbol{U}(\omega_l,k)Y^*(\omega_l,k)}{P_U(\omega_l,k)},\quad l=1,2,...,L, \tag{23}$$

where

$$P_U(\omega_l,k)=\rho P_U(\omega_l,k-1)+(1-\rho)\sum_{m=1}^{M}\left|\boldsymbol{U}_m(\omega_l,k)\right|^2. \tag{24}$$

$P_U(\omega_l, k)$ denotes the adaptive power estimation of the input noise with a forgetting factor ρ, and μ denotes the step size. The output waveform of the robust GSC is formed using the overlap and add method in Crochiere (1980).

Finally, the two proposed methods are given. The first method (Proposal 1) is listed as follows:

Proposal 1 Given $\gamma, \rho, \mu, \bar{\boldsymbol{a}}(\omega_l, k), \Theta_{\text{SOI}}$

Step 1: Obtain the fixed Beamformer $Y_{\text{FB}}(\omega_l,k)=\boldsymbol{F}^{\text{H}}_{\text{FB}}(\omega_l,k)\boldsymbol{X}(\omega_l,k), l=1, 2,\ldots,L.$

Step 2: Calculate PR_m with Eq. (7), and perform eigenanalysis

$$\begin{cases}\text{PR}_m<\gamma\Rightarrow\boldsymbol{v}_m(\omega_l,k)\in\boldsymbol{U}_{\text{IPN}}(\omega_l,k),\\ \text{PR}_m\geq\gamma\Rightarrow\boldsymbol{v}_m(\omega_l,k)\in\boldsymbol{U}_{\text{SOI}}(\omega_l,k),\end{cases}$$

m=1, 2, …, M, l=1, 2, …, L, to reconstruct $\bar{\boldsymbol{R}}_{\text{IPN}}(\omega_l,k)$ with Eq. (9).

Step 3: Solve Eq. (14) with GEVD to obtain $\boldsymbol{F}_{\text{MaxSINR}}(\omega_l, k)$.

Step 4: Calculate the blocking matrix $\boldsymbol{B}(\omega_l, k)$ with Eqs. (20) and (21), and then obtain the noise reference $\boldsymbol{U}(\omega_l, k)$.

Step 5: Update the multichannel Wiener filter in ANC $\boldsymbol{G}(\omega_l,k+1)=\boldsymbol{G}(\omega_l,k)+\mu\dfrac{\boldsymbol{U}(\omega_l,k)Y^*(\omega_l,k)}{P_U(\omega_l,k)}$, l=1, 2, …, L, and output the enhanced waveform $Y(\omega_l,k)=Y_{\mathrm{FB}}(\omega_l,k)-\boldsymbol{G}^{\mathrm{H}}(\omega_l,k)\boldsymbol{U}(\omega_l,k)$, l=1, 2, …, L.

Step 6: Repeat steps 1–5 until convergence.

The second method (Proposal 2) is set up the same as Proposal 1 except for step 2 where it uses the modified eigenanalysis method (12).

3.4 Complexity of the methods

As the computational burden results mainly from eigenvalue decomposition and GEVD, the proposed methods require $O(M^3)$ computations. The integration method based on the Capon spatial spectrum in Gu and Leshem (2012) has a complexity of $O(SM^2)$, where S is the sampling point in Θ_{IPN} and typically $S\gg M$. The total complexity of this integration method would be $\max\{O(SM^2), O(M^3)\}$ when it is put into our proposed GSC structure. In comparison, the computational complexity of the CBF and standard GSC are $O(M)$ and $O(M^2)$, respectively. In conclusion, the computational complexities of the proposed methods is larger than that of the CBF and the standard GSC, but it is lower than that of the integration method when $S>M$. In addition, the proposed methods have superior performance to the others, including lower signal distortion, higher correlation coefficient with SOI waveform, and higher output SINR.

4 Simulation results

We consider a uniform linear array of M=50 omnidirectional sensors, with a half-wavelength spacing at the highest frequency of the frequency band of interest. One SOI and two interference signals with plane wavefronts are Gaussian white noise with directions 5°, 10°, and 30°, respectively. The background noise is also Gaussian white noise. The random DOA mismatch ϕ_Δ of the SOI is uniformly distributed in [−2°, 2°]. That is, the presumed DOA of the SOI is uniformly distributed in [3°, 7°].

To investigate the ability to cope with a DOA mismatch, the two proposed GSCs are compared to the CBF, the standard GSC in Griffiths and Jim (1982) where $\boldsymbol{B}_{\mathrm{s}}(\omega_l,\bar{\phi}_{\mathrm{SOI}})$ is adopted, and the GSC employing the integration method in Gu and Leshem (2012), for IPN covariance matrix reconstruction. Note that the integration method uses the shrinkage estimation method in Du et al. (2010) to inverse $\bar{\boldsymbol{R}}_X(\omega_l)$ when the number of snapshots is smaller than M. The optimal GSC without DOA mismatch is also considered using the actual SV of the SOI and the exact IPN covariance matrix. For each interference in each sensor, SIR=−10 dB is set to ensure that the output SINR of the CBF is around 0 dB.

Here the assumed DOA of the SOI is in the center of Θ_{SOI} where a mismatch span Θ_Δ is set to include the actual DOA of the SOI while excluding the DOAs of the interference signals. Based on the array structure and the bandwidth of interest, the 3 dB main-lobe bandwidth of the CBF beam pattern is 2°. Thus, the mismatch span Θ_Δ=3° is reasonable. This means that Θ_{SOI} is set to be $(5°+\phi_\Delta-\Theta_\Delta, 5°+\phi_\Delta+\Theta_\Delta)=(2°+\phi_\Delta, 8°+\phi_\Delta)$, and Θ_{IPN} is $[-90°, 2°+\phi_\Delta]\cup[8°+\phi_\Delta, 90°]$. For the two proposed methods, the threshold γ in Eqs. (8) and (12) is assigned a value of 0.7, and η in Eq. (15) is appointed to be 1 without loss of generality. All methods are implemented in the frequency domain with the FFT length of 1024. In the ANC stage, ρ=0.98 and μ=0.01 are chosen.

Three performance measurements are calculated when each method reaches convergence: the correlation coefficient CC between the output waveform $y(i)$ and the input SOI waveform $s(i)$, the output SINR and the signal distortion SD. They are expressed as

$$\mathrm{CC}=\frac{\sum\limits_{i\in T_{\mathrm{o}}}s(i)y(i)}{\sqrt{\sum\limits_{i\in T_{\mathrm{o}}}s^2(i)\sum\limits_{i\in T_{\mathrm{o}}}y^2(i)}}, \tag{25}$$

$$\begin{cases}\mathrm{SINR}_{\mathrm{out}}=10\lg\left(\dfrac{\sum\limits_{i\in T_{\mathrm{o}}}y_{\mathrm{s}}^2(i)}{\sum\limits_{i\in T_{\mathrm{o}}}n_{\mathrm{out}}^2(i)}\right),\\ \mathrm{SD}=10\lg\left(\dfrac{\sum\limits_{i\in T_{\mathrm{o}}}\left(s(i)-y_{\mathrm{s}}(i)\right)^2}{\sum\limits_{i\in T_{\mathrm{o}}}s^2(i)}\right),\end{cases} \tag{26}$$

where i is the time index, T_o is the duration range of the output waveform, and $y_s(i)$ and n_{out} denote the SOI component and IPN component in $y(i)$, respectively. For the variations in the number of snapshots, each sensor is set to have SNR=−10 dB. To compare the performances with different input SNR, the number of snapshots is fixed at K=25. When the number of sensors varies, the fixed DOA mismatch ϕ_Δ=−1.5°, SNR=0 dB, and K=0.5M are assigned. Fifty Monte-Carlo runs are conducted to obtain each point in our simulations.

First, the performance comparisons with regard to the number of snapshots are illustrated in Fig. 2. It is shown that the two proposed GSCs perform better than other techniques tested. They achieve the least SOI distortion, the highest correlation coefficients with the SOI, and the highest output SINR. Specifically, Proposal 2 produces much less signal distortion than Proposal 1, and has the best performance of all. As shown in Fig. 2a, the signal distortion of the proposed methods increases with fewer snapshots. This means that the number of snapshots should be no smaller than 0.5M to control the signal distortion under −10.8 dB. In contrast, when the number of snapshots is smaller than that of the sensors, the integration method fails to work unless it uses a diagonal loading technique or shrinkage estimation method (Du et al., 2010).

Second, we compare the performances for different input SNRs in Fig. 3. It is obvious that the proposed methods outperform the others under a range of low input SNRs. As depicted in Fig. 3a, the integration method and the standard GSC produce distortion increasingly as the input SNR increases, while the proposed methods decrease the distortion gradually. As stated in Section 3.1.1, the integration method uses inaccurate sample covariance matrix estimation $\bar{\boldsymbol{R}}_X(\omega,k)$ to calculate the Capon spatial spectrum. Hence, some SOI power components leak into the integration range Θ_{IPN}, and inaccurate $\bar{\boldsymbol{R}}_{\mathrm{IPN}}(\omega,k)$ reconstruction (containing SOI components) is unavoidable. As this effect becomes more serious when the input SNR increases, the integration method produces more signal distortion. However, the proposed methods can discriminate the SOI and the IPN well in the subspace domain. Proposal 2 can identify and remove the exact eigenvector dominated by the SOI; therefore, IPN covariance matrix reconstruction is accurate and the distortion can be reduced to the lowest. As shown in Figs. 3b–3d, the proposed methods can mitigate the influence of imprecise DOA information to better suppress the IPN and improve the quality of the SOI. Note that there is a gap

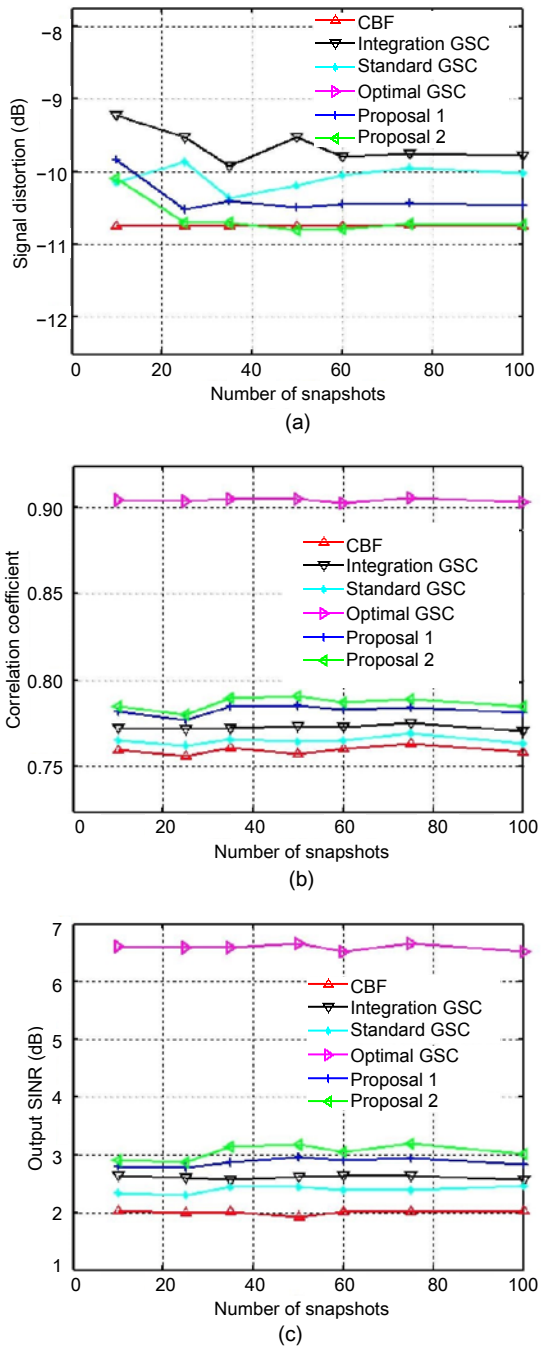

Fig. 2 Performance measurements in terms of the number of snapshots with SNR=−10 dB: (a) signal distortion; (b) correlation coefficients with the SOI; (c) output SINR

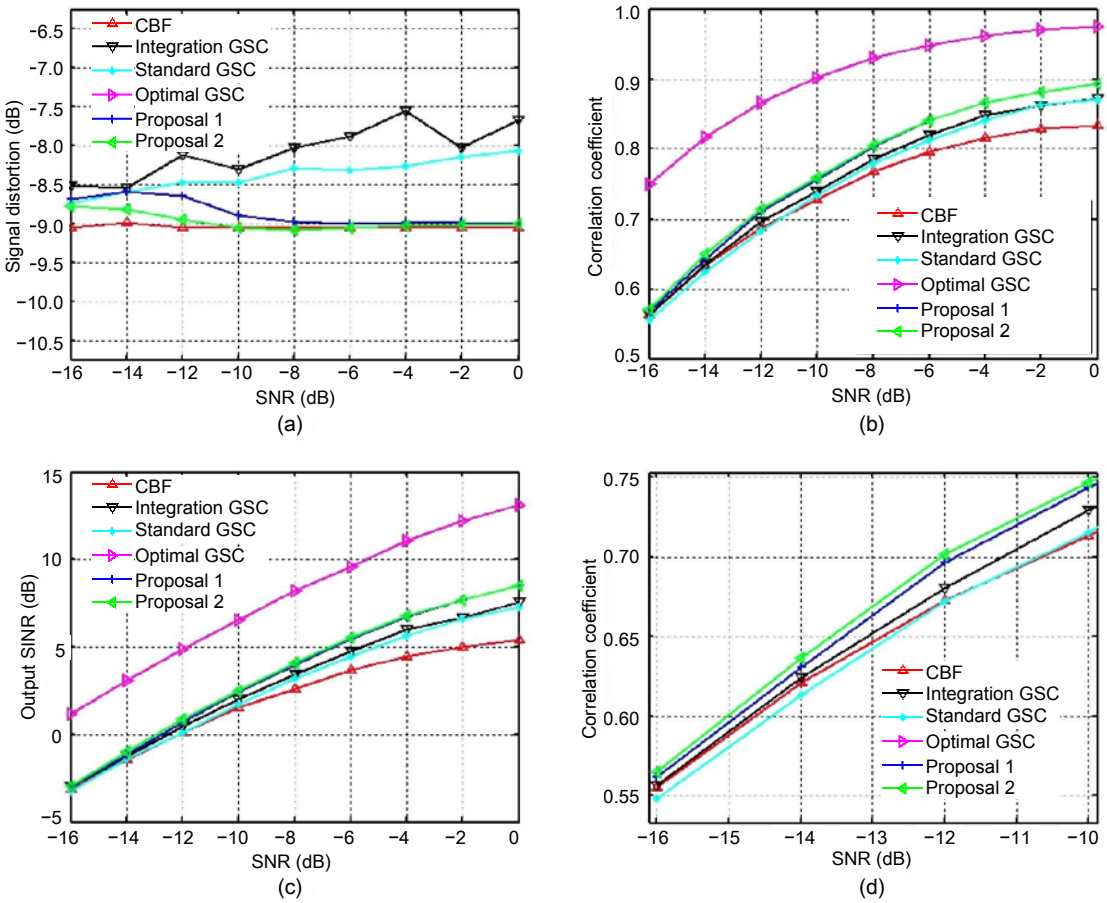

Fig. 3 Performance measurements in terms of the input SNR with K=25: (a) signal distortion; (b) correlation coefficients with the SOI; (c) output SINR; (d) part of (b) in the low SNRs

between the proposed GSCs and the optimal GSC since the DOA of the fixed beamformer is not corrected. However, it does not affect the robustness of the proposed blocking matrices.

Third, the performance measurements with respect to the number of sensors are illustrated in Fig. 4. It is shown in Fig. 4a that the proposed GSCs reach the highest output correlation coefficient, which is always above 0.75. The reason for the performance variations is that the structural characteristics of a CBF beam pattern change with different numbers of sensors when the spacing and frequency band are fixed. To stress the performance difference clearly, we show the performance measurement increments referring to the CBF in Figs. 4b–4d. We can see that the proposed methods outperform the integration method and the CBF. The difference between the proposed methods and the standard GSC becomes more significant as the number of sensors increases. In general, the correlation coefficient between the steering vector of the interference and the SOI cannot be seen as zero. When the bearing interval between the adjacent interference and the SOI is very small, the SOI subspace and the interference subspace cannot be separated thoroughly. This will influence the result of eigenvalue decomposition on the sample covariance matrix, which is based on orthogonality. Thus, given a small number of sensors, the proposed two GSCs perform as well as the standard GSC with regard to the output CC and $\mathrm{SINR}_{\mathrm{out}}$. With a larger number of sensors, the array resolution increases, while the correlation coefficient between the SOI and the interference decreases. The standard GSC becomes more sensitive to the DOA mismatch, and at the same time, the proposed methods improve the robustness due to the more precise IPN estimation.

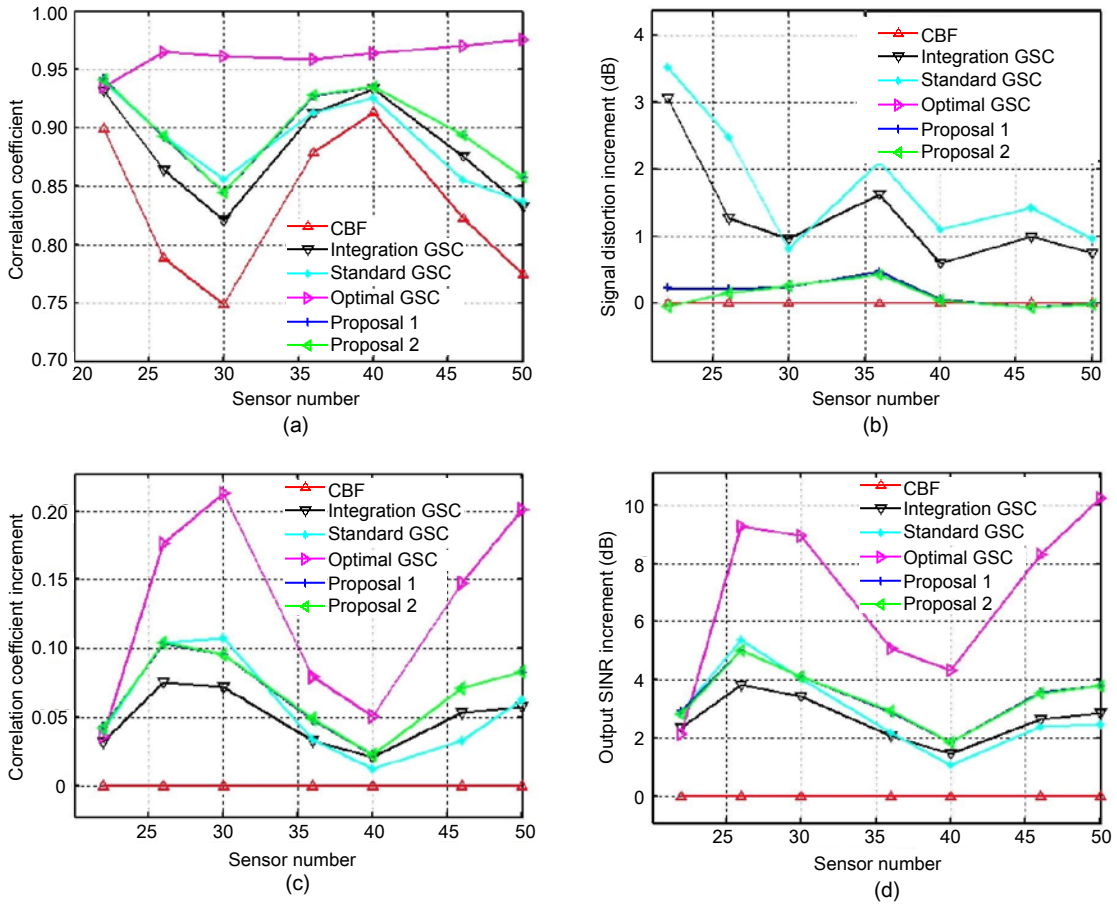

Fig. 4 Performance comparisons in terms of the number of sensors when SNR=0 dB and K=0.5M: (a) correlation coefficients with the SOI; (b) signal distortion increments referring to the CBF; (c) correlation coefficient increments referring to the CBF; (d) output SINR increments referring to the CBF

5 Conclusions

In this paper, a GSC structure which is robust to DOA mismatch with an eigenanalysis-based blocking matrix is proposed. The key idea is to reconstruct the IPN covariance matrix with the basic eigenanalysis method and its modified method. The latter is based on the rank-one assumption to remove the SOI subspace precisely and adaptively. The covariance matrix extracted is incorporated into the MaxSINR beamformer for the subsequent blocking matrix construction. Then the robust blocking matrix is obtained by projecting the MaxSINR beamformer weight vector to the IPN subspace. It can minimize the SOI leakage and in the meantime maximize the noise and interference power in the noise reference, which is provided for an NLMS-based ANC to obtain the enhanced waveform. Simulation results demonstrate that when there exists a DOA mismatch, the proposed GSCs not only remarkably decrease the amount of signal distortion, but also achieve considerable improvements in terms of the output SINR and correlation coefficients with the desired signal, especially with large numbers of sensors. In addition, it can work even when the number of snapshots is smaller than that of the sensors. In the future, the correction of the SV of the SOI and the robustness against an array geometry mismatch will be topics for further research.

Compliance with ethics guidelines

Quan-dong WANG, Liang-hao GUO, Wei-yu ZHANG, Sui-ling REN, and Chao YAN declare that they have no conflict of interest.

References

Buckley K, 1987. Spatial/spectral filtering with linearly constrained minimum variance beamformers. *IEEE Trans Acoust Speech Signal Process*, 35(3):249-266. https://doi.org/10.1109/TASSP.1987.1165142

Capon J, 1969. High-resolution frequency-wavenumber spectrum analysis. *Proc IEEE*, 57(8):1408-1418. https://doi.org/10.1109/PROC.1969.7278

Chen FF, Shen F, Song JY, 2015. Robust adaptive beamforming using low-complexity correlation coefficient calculation algorithms. *Electron Lett*, 51(6):443-445. https://doi.org/10.1049/el.2015.0263

Chen P, Zhao YJ, Liu CC, 2016. Robust adaptive beamforming using a low-complexity steering vector estimation and covariance matrix reconstruction algorithm. *Int J Antenn Propag*, 2016:2438183. https://doi.org/10.1155/2016/2438183

Cornelis B, Moonen M, Wouters J, 2011. Performance analysis of multichannel Wiener filter-based noise reduction in hearing aids under second order statistics estimation errors. *IEEE Trans Audio Speech Lang Process*, 19(5): 1368-1381. https://doi.org/10.1109/TASL.2010.2090519

Crochiere R, 1980. A weighted overlap-add method of short-time Fourier analysis/synthesis. *IEEE Trans Acoust Speech Signal Process*, 28(1):99-102. https://doi.org/10.1109/TASSP.1980.1163353

Doclo S, Spriet A, Wouters J, et al., 2007. Frequency-domain criterion for the speech distortion weighted multichannel Wiener filter for robust noise reduction. *Speech Commun*, 49(7-8):636-656. https://doi.org/10.1016/j.specom.2007.02.001

Du L, Li J, Stoica P, 2010. Fully automatic computation of diagonal loading levels for robust adaptive beamforming. *IEEE Trans Aerosp Electron Syst*, 46(1):449-458. https://doi.org/10.1109/TAES.2010.5417174

Feldman DD, 1996. An analysis of the projection method for robust adaptive beamforming. *IEEE Trans Antenn Propag*, 44(7):1023-1030. https://doi.org/10.1109/8.504311

Gannot S, Burshtein D, Weinstein E, 2001. Signal enhancement using beamforming and nonstationarity with applications to speech. *IEEE Trans Signal Process*, 49(8): 1614-1626. https://doi.org/10.1109/78.934132

Gong YY, Wang L, Yao RG, et al., 2017. A robust method to suppress jamming for GNSS array antenna based on reconstruction of sample covariance matrix. *Int J Antenn Propag*, 2017:9764283. https://doi.org/10.1155/2017/9764283

Griffiths L, Jim C, 1982. An alternative approach to linearly constrained adaptive beamforming. *IEEE Trans Antenn Propag*, 30(1):27-34. https://doi.org/10.1109/TAP.1982.1142739

Gu Y, Leshem A, 2012. Robust adaptive beamforming based on interference covariance matrix reconstruction and steering vector estimation. *IEEE Trans Signal Process*, 60(7):3881-3885. https://doi.org/10.1109/TSP.2012.2194289

Gu YJ, Goodman NA., Hong SH, et al., 2014. Robust adaptive beamforming based on interference covariance matrix sparse reconstruction. *Signal Process*, 96:375-381. https://doi.org/10.1016/j.sigpro.2013.10.009

Habets EAP, Benesty J, 2013. Multi-microphone noise reduction based on orthogonal noise signal decompositions. *IEEE Trans Audio Speech Lang Process*, 21(6):1123-1133. https://doi.org/10.1109/TASL.2013.2244086

Haykin S, 2010. Adaptive Filter Theory (4th Ed.). Publishing House of Electronics Industry, Beijing, China (in Chinese).

Herbordt W, Kellermann W, 2002. Analysis of blocking matrices for generalized sidelobe cancellers for non-stationary broadband signals. Proc IEEE Int Conf on Acoustic Speech Signal Processing, p.IV-4187. https://doi.org/10.1109/ICASSP.2002.5745662

Hoshuyama O, Sugiyama A, Hirano A, 1999. A robust adaptive beamformer for microphone arrays with a blocking matrix using constrained adaptive filters. *IEEE Trans Signal Process*, 47(10):2677-2684. https://doi.org/10.1109/78.790650

Huang F, Sheng W, Ma XF, 2012. Modified projection approach for robust adaptive array beamforming. *Signal Process*, 92(7):1758-1763. https://doi.org/10.1016/j.sigpro.2012.01.015

Huang L, Zhang J, Xu X, et al., 2015. Robust adaptive beamforming with a novel interference-plus-noise covariance matrix reconstruction method. *IEEE Trans Signal Process*, 63(7):1643-1650. https://doi.org/10.1109/TSP.2015.2396002

Jia WM, Jin W, Zhou SH, et al., 2013. Robust adaptive beamforming based on a new steering vector estimation algorithm *Signal Process*, 93(9):2539-2542. https://doi.org/10.1016/j.sigpro.2013.03.015

Li J, Stoica P, 2005. Robust Adaptive Beamforming. John Wiley & Sons, New York, USA.

Li WX, Mao XJ, Zhai ZQ, et al., 2016. High performance robust adaptive beamforming in the presence of array imperfections. *Int J Antenn Propag*, 2016:3743509. https://doi.org/10.1155/2016/3743509

Qian JH, He ZS, Xie JL, et al., 2017. Null broadening adaptive beamforming based on covariance matrix reconstruction and similarity constraint. *EURASIP J Adv Signal Process*, 2017:1. https://doi.org/10.1186/s13634-016-0440-1

Ren SL, Ge FX, Guo X, et al., 2015. Eigenanalysis-based adaptive interference suppression and its application in acoustic source range estimation. *IEEE J Ocean Eng*, 40(4):903-916. https://doi.org/10.1109/JOE.2014.2359378

Shen F, Chen FF, Song JY, 2015. Robust adaptive beamforming based on steering vector estimation and covariance matrix reconstruction. *IEEE Commun Lett*, 19(9):1636-1639. https://doi.org/10.1109/LCOMM.2015.2455503

Souden M, Benesty J, Affes S, 2010. On optimal frequency-domain multichannel linear filtering for noise reduction. *IEEE Trans Audio Speech Lang Process*, 18(2):260-276. https://doi.org/10.1109/tasl.2009.2025790

Spriet A, Moonen M, Wouters J, 2004. Spatially pre-processed speech distortion weighted multi-channel Wiener filtering for noise reduction. *Signal Process*, 84(12):2367-2387. https://doi.org/10.1016/J.SIGPRO.2004.07.028

Talmon R, Cohen I, Gannot S, 2009. Convolutive transfer function generalized sidelobe canceler. *IEEE Trans Audio Speech Lang Process*, 17(7):1420-1434. https://doi.org/10.1109/TASL.2009.2020891

van Trees HL, 2002. Optimum array processing. In: Detection, Estimation, and Modulation Theory, Part IV. Wiley & Sons, New York, NY, USA.

Wang L, Gerkmann T, Doclo S, 2015. Noise power spectral density estimation using MaxNSR blocking matrix. *IEEE/ACM Trans Audio Speech Lang Process*, 23(9): 1493-1508. https://doi.org/10.1109/TASLP.2015.2438542

Wang Y, Bao QL, Chen, ZP, 2016. Robust adaptive beamforming using IAA-based interference-plus-noise covariance matrix reconstruction. *Electron Lett*, 52(13):1185-1186. https://doi.org/10.1049/el.2015.4420

Warsitz E, Haeb-Umbach R, 2007. Blind acoustic beamforming based on generalized eigenvalue decomposition. *IEEE Trans Audio Speech Lang Process*, 15(5):1529-1539. https://doi.org/10.1109/TASL.2007.898454

Warsitz E, Krueger A, Haeb-Umbach R, 2008. Speech enhancement with a new generalized eigenvector blocking matrix for application in a generalized sidelobe canceller. Proc IEEE Int Conf on Acoustic Speech Signal Processing, p.73-76. https://doi.org/10.1109/ICASSP.2008.4517549

Yang LC, Qian YT, 2014. Speech enhancement with a GSC-like structure employing sparse coding. *J Zhejiang Univ-Sci C (Comput & Electron)*, 15(12):1154-1163. https://doi.org/10.1631/jzus.C1400085

Yuan X, Gan L, 2016. Robust algorithm against large look direction error for interference-plus-noise covariance matrix reconstruction. *Electron Lett*, 52(6):448-450. https://doi.org/10.1049/el.2015.3716

Yuan XL, Gan L, 2017. Robust adaptive beamforming via a novel subspace method for interference covariance matrix reconstruction. *Signal Process*, 130:233-242. https://doi.org/10.1016/j.sigpro.2016.07.008

Zhang ST, Thng ILJ, 2002. Robust presteering derivative constraints for broadband antenna arrays. *IEEE Trans Signal Process*, 50(1):1-10. https://doi.org/10.1109/78.972477

Zhang YP, Li WJ, Chen Q, et al., 2016. A robust adaptive beamformer based on desired signal covariance matrix estimation. Proc IEEE Int Conf on Signal Processing Communications and Computing, p.1-4. https://doi.org/10.1109/ICSPCC.2016.7753672

Zhang ZY, Liu W, Leng W, et al., 2016. Interference-plus-noise covariance matrix reconstruction via spatial power spectrum sampling for robust adaptive beamforming. *IEEE Signal Process Lett*, 23(1):121-125. https://doi.org/10.1109/LSP.2015.2504954

Zhao Y, Liu W, Langley RJ, 2011. Adaptive wideband beamforming with frequency invariance constraints. *IEEE Trans Antenn Propag*, 59(4):1175-1184. https://doi.org/10.1109/TAP.2011.2110630

Zhu YT, Zhao YB, Liu J, et al., 2016. Low complexity robust adaptive beamforming for general-rank signal model with positive semidefinite constraint. *Front Inform Technol Electron Eng*, 17(11):1245-1252. https://doi.org/10.1631/FITEE.1601112